Fabrication of the 6.5 m primary mirror for the Multiple Mirror Telescope Conversion

H. M. Martin, J. H. Burge, D. A. Ketelsen and S. C. West

Steward Observatory, University of Arizona, Tucson, AZ 85721

ABSTRACT

The Steward Observatory Mirror Lab is in the process of fabricating the 6.5 m mirror for the conversion of the Multiple Mirror Telescope (MMT) to a single primary mirror. For this purpose the Lab has developed a versatile polishing system built around the stressed lap polishing tool. The system must produce an f/1.25 parabolic surface with an accuracy corresponding to 0.09 arcsecond FWHM seeing and 1.5% scattering loss at 500 nm wavelength.

Keywords: telescopes, optical fabrication, optical testing, aspheres

1. INTRODUCTION

The Multiple Mirror Telescope on Mt. Hopkins in southern Arizona is being converted to a single-mirror telescope, the six 1.8 m mirrors replaced by a single 6.5 m primary. When the telescope was originally constructed in the 1970s, technology did not exist to make a mirror of this size and the required quality. The multiple mirror concept gave astronomers one of the world's most powerful telescopes at a fraction of the cost of previous 4-5 m telescopes. Now that the mirror technology does exist, a single mirror provides several advantages, especially a doubling of the collecting area by use of a filled aperture, and a 15-fold increase in field of view to 1°. Because the existing enclosure and much of the telescope structure can be used with minor modification, the enhanced performance is again achieved economically.

The 6.5 m mirror is a honeycomb sandwich, the first of its size cast at the Steward Observatory Mirror Lab.[1] The concave front shell and flat back plate are each about 27 mm thick, and these are separated by 12 mm ribs in a hexagonal pattern with 192 mm spacing. The overall thickness is 0.71 m at the edge. In order to make the new telescope fit in the existing MMT building, this mirror is considerably faster at f/1.25 than other large mirrors. The short focal length is an advantage as well as a necessity, making the structure stiff and giving a large plate scale (1° in 0.6 m) at the f/5 Cassegrain focus without requiring an excessively large secondary. For these reasons, and especially because of the compact and economical enclosure, a number of other projects using honeycomb sandwich mirrors have adopted equal or faster focal ratios.[2,3]

Such fast mirrors present the challenge of polishing the extremely aspheric surface, and the Mirror Lab's polishing system is designed for that purpose. Nearly all lapping operations are performed with a stressed lap that is relatively large (1.2 m) and stiff, and maintains fit through continuous active shape changes.[4,5] Previous experience with the stressed lap included a 1.8 m f/1 primary and three 3.5 m primaries of f/1.5-f/1.75, all honeycomb sandwich mirrors, figured to about 20 nm rms surface and operating successfully in telescopes. The MMT primary is a step up in size and asphericity. The accuracy requirement is stringent also, corresponding to a seeing-limited image size of 0.09 arcsecond FWHM and a scattering loss due to small-scale structure of 1.5% (both at 500 nm wavelength).

2. ACCURACY REQUIREMENTS

The optical error budget for the MMT Conversion is given in terms of the wavefront structure function, often used to characterize the wavefront perturbed by the atmosphere. The structure function D_φ is the mean square phase difference between pairs of points in the aperture as a function of the separation r between those points. Knowledge of the structure function fully determines the long-exposure optical transfer function and point-spread function. Since our goal is to ensure that the telescope does not significantly degrade the best seeing-limited wavefront, we adopt the form of the ideal atmospheric structure function,

$$D_{\varphi}(r) = 7.12\left(\frac{r\theta}{\lambda}\right)^{5/3} \text{rad}^2, \quad (1)$$

with each component of the error budget allocated an image size θ defined as the full width at half maximum. The structure functions of the components add linearly to give the combined structure function.

The primary mirror surface is allowed an error corresponding to seeing of 0.092 arcsecond FWHM at $\lambda = 500$ nm. The ideal atmospheric structure function approaches zero toward small separations. In order to soften this requirement of infinite smoothness, the mirror surface structure function is allowed to approach a constant for small spacings, corresponding to small-scale structure that scatters some fraction of the light over wide angles. The allowed loss for the MMT primary is 1.5% at 500 nm. The structure function can be related to the Central Intensity Ratio used by ESO to specify the VLT optics.[6] If we were to precisely meet the structure function goal, the CIR would be 73% in 0.2 arcsecond seeing. For all previous mirrors polished at the Mirror Lab, the final structure function was significantly below the goal for large spacings, giving a larger CIR.

Accuracy in radius of curvature and conic constant, or spherical aberration, are treated as separate requirements. The allowed error in conic constant is 10^{-4}, corresponding to 82 nm peak-to-valley surface spherical aberration at best focus. The telescope is relatively insensitive to errors in radius of curvature, but the null test of the mirror in the lab is very sensitive to radius errors because they affect the distance from the null lens to the mirror.[7] The allowed error is 1 mm.

3. GENERATING THE PARABOLOID

The Mirror Lab's fabrication process involves three steps: aspheric generating (machining), loose-abrasive grinding, and polishing. These represent a gradual transition to higher accuracy and lower removal rate. All steps are performed by the same machine, the 8.5 m capacity Large Optical Generator (LOG).[8] It uses a cylindrical polar geometry with horizontal and vertical motion of the tool and rotation of the mirror. Several layers of hardware and software safety checks protect the mirror against the possibility of errant commands or failed sensors, especially important during generating when an error could destroy the mirror in a few seconds. The safety features include two separate computers, one to control and one to monitor, two independent encoders for each linear axis, and a displacement sensor to monitor the height of the tool relative to the glass.

Generating serves several functions, some of them unique to structured mirrors. It finalizes the mechanical geometry, including thicknesses and wedges of front and back plates and mechanical axis of symmetry. It approximately fixes the optical axis of the paraboloid, although this can be translated a few mm if necessary by introducing coma during loose-abrasive grinding. And it should produce an aspheric surface accurate to around 10 microns rms with limited subsurface damage.

We generated the back surface first, using as a support the same steel frame to which the mirror had been attached since it was lifted from the furnace. We chose the mechanical axis to match the centroid of the honeycomb structure and to minimize wedge in the two faceplates. The mirror contains 1020 hexagonal cells (voids) on 192 mm spacing and separated by ribs 12 mm wide. We measured the positions of 84 uniformly spaced rib intersections by viewing them through the front surface with a CCD camera mounted on the generating spindle, and using the LOG's encoders to measure position. Uncertainty is dominated by random local variations in mirror geometry, about 0.5 mm rms in each coordinate; by averaging we were able to define the centroid to better than 0.1 mm rms. We made cylindrical cuts at the edges of front and back plates with the mirror centered according to these measurements.

After verifying that the cast internal surfaces of the front and back plates were parallel within a few tenths of a mm across the 6.5 m diameter, we measured the thickness of the back plate with an ultrasonic gauge at 60 equally spaced cells, and adjusted tilt to minimize wedge in these measurements. We reduced the thickness from about 30 mm to 26.5 mm with less than 0.2 mm of wedge. We then lapped and polished the surface, in order both to strengthen it and to allow inspection of the internal structure.

After turning the mirror over and mounting it on hydraulic supports (described in the next section), we generated the parabolic optical surface, removing about 5 mm of glass to a final thickness of 27 mm. Near the end of this process it was necessary to fill 43 bubbles of 15-30 mm diameter that would intersect the optical surface. These bubbles were present because the

glass was not kept molten long enough in this first casting of a mirror this size. We ground the bubbles to near hemispheres of three standard sizes (19, 25 and 32 mm) and made matching hemispherical plugs out of identical borosilicate glass. We epoxied the plugs into the holes after lapping the surfaces together down to a 12 micron abrasive. One plug appeared to debond partially, and was ground out and replaced. One year after installation of the plugs, glue bonds can be seen only with difficulty in the polished surface. The plugs create no surface features or figure errors detectable with a 10.6 micron interferometer, i. e. greater than 100 nm. Smaller figure errors will not be detectable until the visible interferometer is installed.

We measured the generated surface using the LOG as a profilometer, with a probe mounted on the generating spindle. This left us vulnerable to errors in the motion of the spindle and turntable bearing--errors that would be common to generating and measurement--a risk deemed acceptable at this early stage. We calibrated the straightness of the linear axes with a granite straightedge and their scale with a distance-measuring interferometer, but neglected to test the turntable bearing under the 20 ton load of mirror and support cell. The final radial profiles showed figure errors of 50 microns peak-to-valley over the inner 6.2 m, and the outer edge low by 100 microns. At the completion of generating we lapped the surface briefly with 20 micron abrasive and measured the figure with a 10.6 micron interferometer. This verified the radial profile measured by the LOG, but showed that there was in fact an azimuthal error with 120° symmetry and magnitude 100 microns peak-to-valley. Subsequent investigations determined that this error had occurred because the 2-m-diameter turntable bearing was flexing non-uniformly by about 30 microns under the load, which was supported largely at three points. Rather than return to generating, we decided to remove this error by loose-abrasive grinding as described below, with little impact on the ultimate accuracy or schedule.

4. MIRROR SUPPORT

Any safe support is adequate while generating and polishing the back surface, because of the loose tolerances on figure. The optical surface, however, must be figured with the mirror supported approximately as it will be in the telescope. We installed the mirror on its final polishing support prior to generating the front surface. This support system consists of 104 actuators, most of which apply their forces to two or three positions on the mirror through load spreaders.[9] The telescope actuators will be active pneumatic cylinders, while the polishing supports are passive hydraulic cylinders applying the same nominal forces. Each actuator's force is measured by a load cell, and the polishing forces can be adjusted by trim weights if necessary. In anticipation of the active control of low-order bending modes in the telescope, we have the option of removing low-order aberrations measured during polishing, either by software or mechanically via the trim weights.

The load spreaders are steel structures permanently bonded to the polished back surface with silicone adhesive. Their locations must match those of the actuators in the telescope's support cell to high accuracy, the error budget for alignment allowing 0.5 mm rms error in positioning the load spreaders. We located the load spreaders by grinding small, shallow marks (two per load spreader to define position and orientation) on the back surface of the mirror, using a die grinder attached to the generating spindle. We aligned the load spreaders visually to the marks before bonding them. A subsequent survey verified the accuracy of better than 0.5 mm rms.

5. LAPPING OPERATIONS

While the mechanical structure of the LOG serves well for both generating and lapping (loose-abrasive grinding and polishing), the requirements of motion control are at opposite ends of the spectrum. Generating requires slow linear motion, on the order of 0.01-0.1 mm/s, and positioning accuracy of a few microns, while lapping requires speeds up to 100 mm/s and positioning accuracy of about 1 mm. We therefore change linear motors between the two operations, in addition to replacing the generating spindle with the stressed lap and its rotation drive.

All lapping operations use the same stressed lap, comprising a 1.5 m aluminum plate 50 mm thick and 18 moment-generating actuators around the edge of the plate to bend it elastically. Three more actuators apply lifting forces to control polishing pressure and pressure gradients. The polishing surface is 1.2 m in diameter. The full weight corresponds to a pressure of 4700 Pa (0.7 psi) and sets an upper limit to polishing pressure. The bending actuators are programmed to make the lap shape match the ideal parabolic mirror surface at all times, while the lifting actuators can be used to vary the pressure according to the current figure error—applying more pressure at the high points—and to balance forces when the lap extends over the edge of the mirror, a common situation.

The LOG provides dynamic control of the speeds of its three polishing motions (radial, mirror rotation and lap rotation). We generally use the radial motion and lap rotation to control axisymmetric figure errors. Variations in pressure and mirror rotation rate remove non-axisymmetric errors that would be difficult to handle with some more traditional polishing machines. Loose-abrasive grinding and polishing involve the same sorts of tool motion. For loose-abrasive grinding we place aluminum grinding pads 0.5 mm thick on the pitch lap, rather than the traditional ceramic tiles. This is done because active bending of the lap creates the possibility of a substantial shape error in certain failure modes, and the resulting concentrated loads might damage the mirror if applied by ceramic. As we approach the final accuracy we will control mechanical quilting of the honeycomb structure under polishing pressure, by applying an equal air pressure to the inside of the mirror. This strategy was effective in figuring the 3.5 m primary of the WIYN telescope.[10]

Starting loose-abrasive grinding in October 1995, we first concentrated on the trefoil error, using variations in pressure and mirror rotation rate to achieve a dynamic range in removal rate of about 20. After 8 weeks and 140 hours of grinding, this error was essentially eliminated, as was the low edge. The overall surface error had been reduced from about 20 microns to 0.6 microns rms. We started polishing the mirror in January 1996. As of April the rms surface error was 160 nm rms as measured with the IR interferometer.

6. OPTICAL MEASUREMENT

All lapping operations are guided by phase-shifting interferometry. We use a 10.6 micron interferometer for loose-abrasive grinding and early polishing, and a 531 nm interferometer for the final figuring. Both interferometers are sensitive to surface errors of about $\lambda/100$. Separate IR and visible null lenses correct the 820 micron departure from the best-fitting sphere. We verified the accuracy of both null lenses using small computer-generated holograms that mimic the ideal primary mirror.[7]

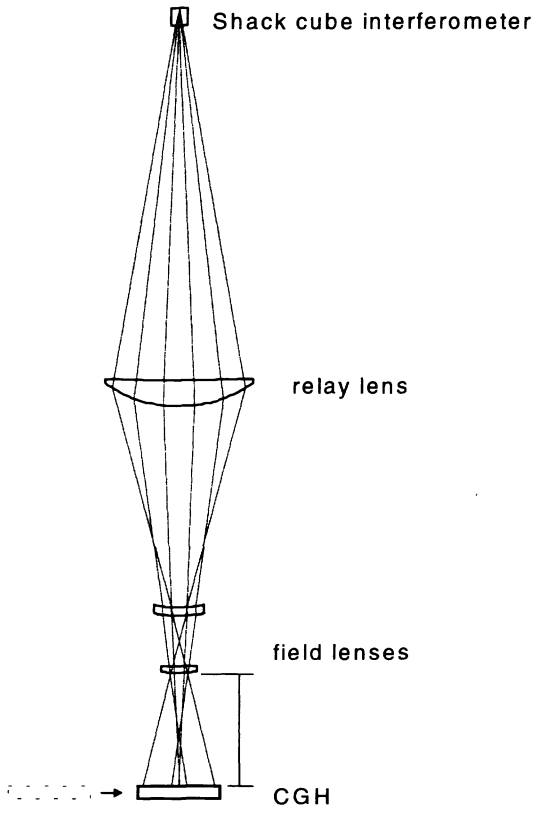

FIGURE 1. Method of verifying the accuracy of the visible null lens. A computer-generated hologram, placed at the paraxial center of curvature, mimics the primary mirror.

The technique for verification is shown in Figure 1. The hologram, a set of reflective rings on flat glass, is placed at the paraxial center of curvature of the primary mirror, just below the null lens. It is designed and made, independently of the null lens, to match the wavefront that would propagate to coincide with the surface of the primary mirror. We measure this hologram exactly as we measure the primary, aligning the interferometer and null lens simply by translating and tilting them as a rigid body to eliminate power, tilt and coma. Any wavefront error obtained in this measurement could represent an error in either the hologram or the null lens, but we can infer with confidence that the null lens is at least as accurate as the measured wavefront.

In accordance with the mirror specification, we divide potential errors in the null lens into spherical aberration and residual figure errors. Figure 2 shows the holographic test of the visible null lens. The measured spherical aberration is 16 nm peak-to-valley surface at best focus, corresponding to an error in conic constant of 2×10^{-5}, and the residual surface error is 12 nm rms. These results are consistent with the expected errors in both the null lens and the hologram, and are within the tolerance for measurement of the primary mirror. Our initial holographic measurement of the visible null lens revealed spherical aberration of 1.9 microns. An investigation turned up an error in the null lens: the refractive index of the large element was in error due to incorrect interpretation of the melt data. We corrected the error to high accuracy by respacing the elements. Without the holographic test of the null lens, this error would have been polished into the mirror.

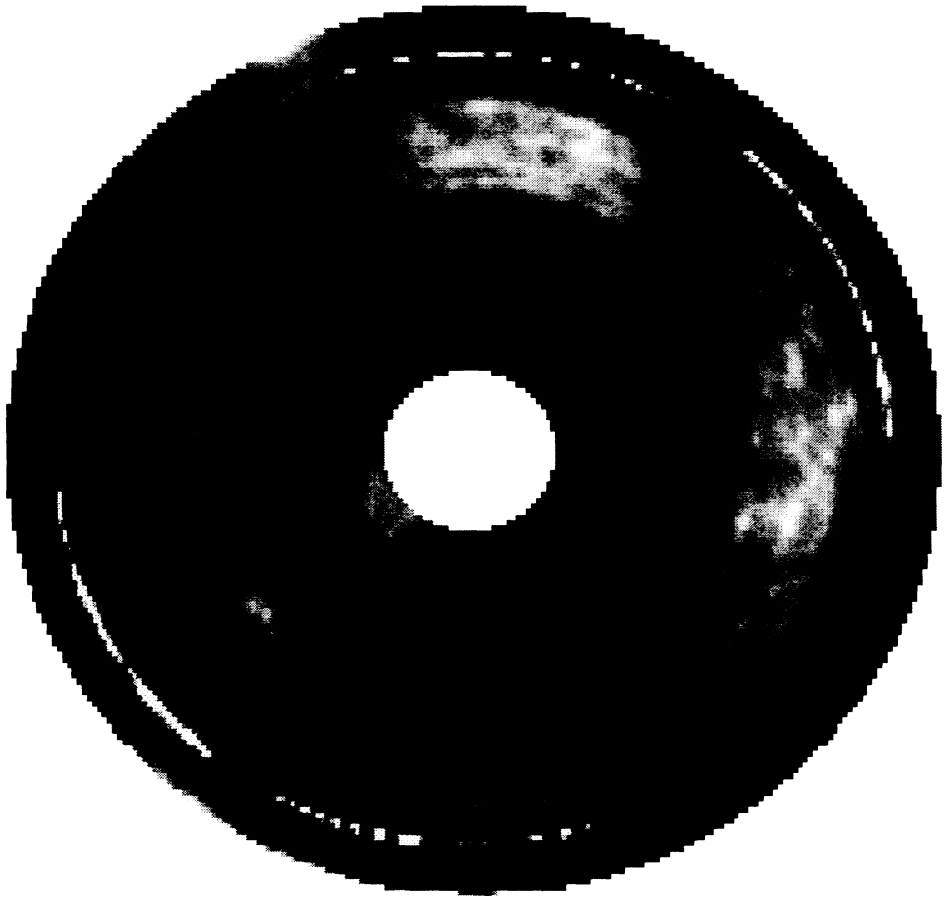

FIGURE 2. Gray-scale map of the surface error obtained from measurement of the hologram with the visible interferometer and null lens. The measured error corresponds to an error of 2×10^{-5} in conic constant and a residual surface error of 12 nm rms, both within the tolerances for measurement error. The gray scale covers the range -50 nm (black) to 50 nm (white) in surface error. Some of the discrete steps are understood to be flaws in the hologram.

7. CONCLUSION

We have developed a versatile generating and polishing system built around the stressed lap. We anticipate meeting the accuracy requirements of matching 0.09 arcsecond seeing and scattering less than 1.5% of light at 500 nm. The MMT primary will be followed by an identical mirror for the Magellan Telescope in Chile, then the first of two 8.4 m f/1.14 mirrors for the Large Binocular Telescope in Arizona.

8. REFERENCES

1. B. H. Olbert, J. R. P. Angel, J. M. Hill, S. F. Hinman, "Casting 6.5-meter mirrors for the MMT conversion and Magellan", in *Advanced Technology Optical Telescopes V*, Larry M. Stepp, Editor, Proc. SPIE 2199, p. 144 (1994).
2. M. J. de Jonge, "Status of the Magellan Project", *ibid*, p. 22.
3. J. M. Hill, P. Salinari, "Optomechanics of the Large Binocular Telescope", *ibid*, p. 64.

4. H. M. Martin, D. S. Anderson, J. R. P. Angel, R. H. Nagel, S. C. West, R. S. Young, "Progress in the stressed-lap polishing of a 1.8-m f/1 mirror", in *Advanced Technology Optical Telescopes IV*, Lawrence D. Barr, Editor, Proc. SPIE 1236, p. 682 (1990).

5. H. M. Martin, D. S. Anderson, J. R. P. Angel, J. H. Burge, W. B. Davison, S. T. DeRigne, B. B. Hille, D. A. Ketelsen, W. C. Kittrell, R. McMillan, R. H. Nagel, T. J. Trebisky, S. C. West, R. S. Young, "Stressed-Lap Polishing of 1.8-m f/1 and 3.5-m f/1.5 Primary Mirrors", in *Proc. ESO Conference on Progress in Telescope and Instrumentation Technologies*, M.-H. Ulrich, Editor, p. 169 (1992).

6. P. Dierickx, "Error budget and expected performance of the VLT unit telescopes", in *Advanced Technology Optical Telescopes V*, Larry M. Stepp, Editor, Proc. SPIE 2199, p. 950 (1994).

7. J. H. Burge, D. S. Anderson, D. A. Ketelsen, S. C. West, "Null test optics for the MMT and Magellan 6.5-m f/1.25 primary mirrors", ibid, p. 658.

8. D. A. Ketelsen, W. B. Davison, S. T. DeRigne, W. C. Kittrell, "Machine for complete fabrication of 8-m class mirrors", *ibid*, p. 651.

9. P. M. Gray, J. M. Hill, W. B. Davison, S. Callahan, J. T. Williams, "Support of large borosilicate honeycomb mirrors", *ibid*, p. 691.

10. D. S. Anderson, H. M. Martin, J. H. Burge, D. A. Ketelsen, S. C. West, "Rapid fabrication strategies for primary and secondary mirrors at the Steward Observatory Mirror Laboratory", *ibid*, p. 199.